Physics and Chemistry of the Earth 34 (2009) 225–235

Contents lists available at ScienceDirect

Physics and Chemistry of the Earth

journal homepage: www.elsevier.com/locate/pce

Water balance estimation of a poorly gauged catchment in West Africa using dynamically downscaled meteorological fields and remote sensing information

Sven Wagner [a,*], Harald Kunstmann [a], A. Bárdossy [b], C. Conrad [c], R.R. Colditz [c]

[a] Forschungszentrum Karlsruhe, Institute for Meteorology and Climate Research IMK-IFU, Kreuzeckbahnstraße 19, 82467 Garmisch-Partenkirchen, Germany
[b] Institute for Hydraulic Engineering, University of Stuttgart, Germany
[c] Department of Geography, University of Wuerzburg, Germany

ARTICLE INFO

Article history:
Received 26 November 2007
Received in revised form 27 March 2008
Accepted 2 April 2008
Available online 20 April 2008

Keywords:
Joint meteorological–hydrological simulations
MM5
TRMM
MODIS
Decision support
Western Africa
Volta basin

ABSTRACT

Scientifically sound decisions in sustainable water management are usually based on hydrological modeling which can only be accomplished by meteorological driving information. Especially in regions with weak infrastructure this task is hampered by limited hydro-meteorological information in sufficient spatial and temporal resolution. We investigated three approaches to provide required meteorological fields driving the distributed hydrological model: the results of the mesoscale meteorological model MM5 which are available near real time, the TRMM product 3B42 available with approximately one month delay, and station data available with a delay of one year or more. The study site is the White Volta catchment in the semi-arid environment of West Africa. The results for 2004 show that the meteorological model is able to provide meteorological input data for near real time water balance estimations. In this study the TRMM product does not improve the simulation results. Besides missing important meteorological data, also gridded information on land surface properties (albedo, LAI, etc.) is usually difficult to obtain, albeit it is an essential input for distributed hydrological models. This information is commonly taken from "static" tables depending on the land use. Satellite remote sensing provides worldwide spatially detailed information on land surface properties which is particularly suitable for large regions in remote settings. Therefore the MODIS products for albedo and LAI were processed to annual time series including the identification and replacement of low quality observations by interpolation. The impact using MODIS data on the spatial distribution of water balance variables occurs mainly on local scale. The hydrological simulations using MODIS LAI and albedo values result in higher annual evapotranspiration and lower total discharge sums for 2004. Altogether it is concluded that hydrological decision support systems in regions with weak infrastructure can benefit significantly from the integration of atmospheric modeling and satellite-derived land surface data.

1. Introduction

Sustainable decisions in water resources management require scientifically sound information on water availability, which includes the quantification of the spatial and temporal changes of water balance variables. Central support in hydrological decision making arises from hydrological modeling which, in turn, depends on meteorological input. In poorly gauged basins this task is hampered by the fact that only little hydro-meteorological information is available. Station data are only available with a considerable temporal delay and therefore unsuitable for specific questions in water resources management, where basin-wide near real time and short-term monitoring is required to support stakeholders and water management authorities in operational irrigation water supply or running hydro-power strategies. Therefore other data sources for the meteorological driving information for hydrological simulations have to be used. In this study three data sources, available with different temporal delay, are applied with a special focus on precipitation, which is the basic component of the water balance. For near real time estimations the hydrological simulations are driven by the output of the mesoscale meteorological model MM5. The integration of atmospheric sciences and hydrology for the development of decision support systems in sustainable water management was performed by Kunstmann et al. (2007) for the Volta basin. Furthermore, this technique was applied by, e.g. Marx (2007) and Kleinn (2002) for catchments in Europe. Using joint atmospheric–hydrological simulations, the water balance estimations are available within two days. The second data source is a product of the Tropical Rainfall Measuring Mission (TRMM) which is available with approximately one month delay. Station data are used as a third

* Corresponding author.
E-mail address: sven.wagner@imk.fzk.de (S. Wagner).

1474-7065/$ - see front matter © 2008 Elsevier Ltd. All rights reserved.
doi:10.1016/j.pce.2008.04.002

meteorological data source. Especially in regions with weak infrastructure, where no automatic data recorders are used, the delay can increase up to one year or more until data are collected, digitized, and become available to the public.

Independent of the meteorologically driving data, land surface properties, like albedo and leaf area index (LAI), are essential input data for distributed hydrological modeling. This information is usually taken from standard literature values and incorporated into hydrological modeling through tables depending on the land use. But standard literature values can be imprecise, especially in regions with few field measurements. In particular in such regions, satellite-based data can improve the available information on land surface properties. Space-borne remote sensing systems such as MODerate resolution Imaging Spectroradiometer (MODIS) acquire full global coverage within 1–2 days. A large suite of land surface properties is made available free of charge as composites of daily, 8-day, or 16-day periods with a spatial resolution of 1000 m or less. Remote sensing techniques in hydrological studies and water resources management for the quantification of surface parameters are used in several studies. For example, Chen et al. (2005) used remote sensing data to characterize the distributions of vegetation types and LAI. Sandholt et al. (2003) integrated vegetation dynamics from remote sensing data in a distributed hydrological model for the Senegal river basin. In this study the MODIS products of the leaf area index (LAI, MOD15A2) and albedo (MOD43B3) are imported into the hydrological model and simulation results using tabulated literature- and MODIS values are compared.

This work will show the application and performance of hydrological simulations driven first by different meteorological input data sources which are available with specific delays and second by different land surface data sources derived from standard literature and multi-temporal MODIS remote sensing data. The study site is the White Volta catchment in Western Africa and the simulations were exemplarily carried out for the year 2004.

2. The White Volta catchment

The study area is one of the main tributaries of the Volta basin, the White Volta catchment (94,000 km^2) situated upstream of Lake Volta in northern Ghana and Burkina Faso (Fig. 1). Lake Volta is one of the largest artificial lakes in the world, and hydropower generation at the Akosombo dam is the major energy source in Ghana. In the basin rain-fed agriculture is the major source of livelihood. Due to increasing demographic pressure, the demand for water, food production, and energy increases continuously, which intensifies the competition for water resources. However, not the precipitation rate itself but also its variability determines the living in this area.

In general, precipitation intensities and total annual rainfall show a strong inter-annual and inter-decadal variability in Western Africa (Hayward and Oguntoyinbo, 1987). Mean annual precipitation in the White Volta catchment ranges from less than 500 mm (North) to more than 1500 mm in the South, of which around 80% occurs between July and September. The spatial precipitation distribution in the White Volta catchment is characterized by a strong latitudinal dependence. Furthermore, small-scale rainfall variability is very high. Friesen (2003) estimated the coefficient of variation of 9×9 km^2 intra-scale rainfall variability to be between 0.25 and 0.4 in northern Ghana. The main agro-ecological zones of the White Volta catchment include the Sudan Savannah (400–1000 mm year^{-1} precipitation) in the northern and Guinea Savannah (around 1200 mm year^{-1} precipitation) in the southern part of the catchment, both with a rainy season from May to October. Climatologically, the White Volta catchment is situated in the semi-arid climate zone with a mean annual temperature between 27 and 36 °C. The mean annual potential evaporation ranges between 2500 mm in the North and 1500 mm in the South. Approximately 80% of the precipitation is lost to evapotranspiration during the rainy season (Oguntunde, 2004).

The topography of the White Volta catchment is very flat, in particular in the southern part (<0.1%). The main geological systems of the catchment are a Precambrian platform and a sedimentary layer. The predominant soil types are lixisols in the southern and arenosols in the northern part (VBRP, 2002). Since 1993, the natural flow regime of the White Volta catchment has been disturbed by a dam and hydropower generation in Bagré in southern Burkina Faso. Due to the strong dependence of downstream hydrographs on the management strategies of the Bagré dam, the simulated runoff was replaced by the measured runoff at the next gauging station in Yarugu to avoid the transmission of errors to the downstream catchments. For this reason and data availability,

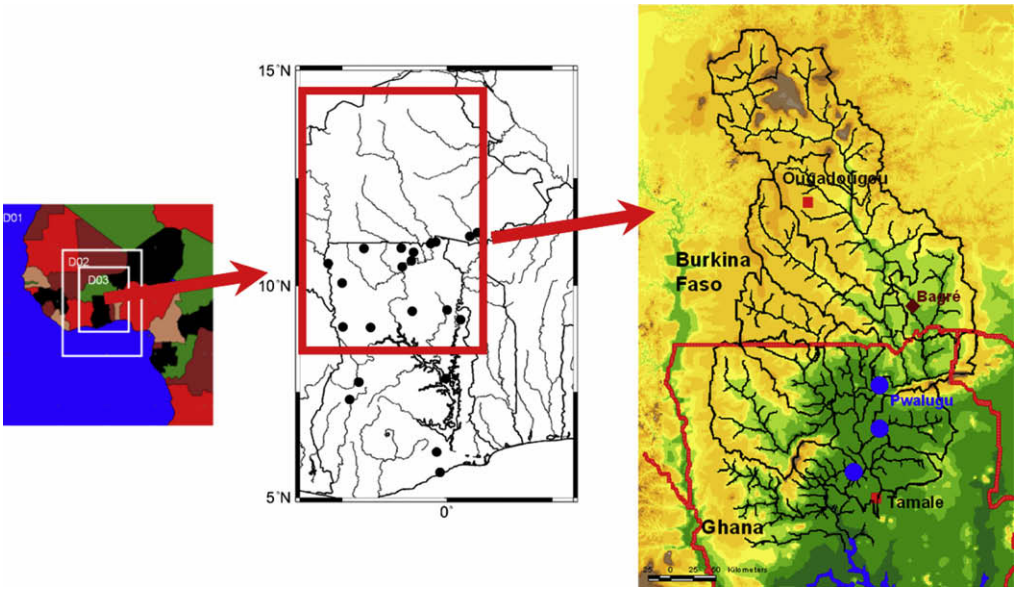

Fig. 1. Nesting strategy for the meteorological modeling (left), location of the 22 available meteorological stations (centre) and set-up of the White Volta catchment for the hydrological simulations (right).

the study focuses on the Ghanaian part of the White Volta catchment.

3. Hydrological model – WaSiM-ETH

For the hydrological simulations the water balance simulation model WaSiM-ETH (Schulla and Jasper, 2000) was used. It is a deterministic, fully distributed modular model for the simulation of the terrestrial water balance using physically-based algorithms for the vertical fluxes. For instance, soil moisture in the unsaturated zone is calculated with the Richards equation (Richards, 1931) and the potential evapotranspiration according to Penman–Monteith (Monteith, 1975). Actual evapotranspiration is estimated using a relation between soil moisture and actual capillary pressure. Groundwater fluxes are calculated by a two-dimensional flow model which is dynamically coupled to the unsaturated zone. Other lateral fluxes like direct runoff and interflow are treated in a lumped manner. Surface runoff is routed to the sub-catchment outlet using a subdivision of the catchment into flow time zones. For considering retention, a single linear storage approach is applied to the surface runoff in the last flow time zone. Translation and retention of interflow is treated accordingly. Discharge routing in the river bed channel is based on a kinematic wave approach.

For the simulations, the White Volta catchment was subdivided into 15 sub-catchments. The outlets of the sub-catchments are mainly located at hydrological stations, such that simulated discharges can be compared with measurements, if available. The outlet of the model set-up is the station Nawuni, the last available station before the White Volta flows into Lake Volta. The spatial resolution of this study is 1×1 km^2 which results in a regular grid of 411×631 grid points. Vertically, the soil is represented by 20 layers with a thickness of 1 m each. The model requires digital elevation data, gridded soil properties (derived from the global FAO soil map), land use, and hydrogeological information (Martin and van de Giesen, 2005).

The model was calibrated and validated with historical observation data on a daily time step. Due to the fact that WaSiM-ETH was so far not used in a semi-arid environment, long time series of meteorological and hydrological were required for the climatic adaptations and calibration/validation process (see Wagner et al., 2006 and Jung, 2006).

4. Meteorological data sources

If near real time estimations are required, the output of a regional meteorological model is often the only possible data source, especially in poorly gauged basins. For the meteorological simulations the mesoscale meteorological model MM5 (Grell et al., 1994) was applied in non-hydrostatic mode to dynamically downscale the global atmospheric fields stepwise using three domains with horizontal resolutions of 81×81 km^2 (61×61 grid points), 27×27 km^2 (85×67 grid points) and 9×9 km^2 (157×121 grid points) (Fig. 1). For the vertical resolution 25 layers from the surface up to 30 hPa were chosen. Jung and Kunstmann (2007) determined an adequate configuration of the available parameterizations for the Volta basin which was used for this study. These are the OSU-Land-Surface Model (Chen and Dudhia, 2001), the MRF-PBL scheme (Hong and Pan, 1996) for the planetary boundary layer, the convective (i.e. cumulus) parameterization according to Grell et al. (1994), the microphysics according to Reisner et al. (1998) (Mixed Phase Graupel) and the cloud-radiation scheme according to Grell et al. (1994). For this study the MM5 version 3.6 in the one-way nesting approach was used.

The second data source is a product of the Tropical Rainfall Measuring Mission (TRMM) which is available with approximately one month delay but only provides precipitation data. TRMM is a joint mission between NASA and the Japan Aerospace Exploration Agency (JAXA) dedicated to measuring tropical and subtropical rainfall through microwave and visible infrared sensors, and includes space-borne rain radar. The average operating altitude of TRMM is 403 km since August 2001. In this study the TRMM product 3B42 (V6) – TRMM merged high quality (HQ)/infrared (IR) precipitation – is used (e.g. http://trmm.gsfc.nasa.gov/3b42.html; Huffman et al., 1995). These gridded estimates are on a 3-h temporal resolution and a 0.25° by 0.25° spatial resolution in a global belt extending from 50° South to 50° North latitude. The 3B42 estimates are produced by first a combination of the microwave and IR estimates. In a second step these estimates are scaled to match the monthly rain gauge analyses used in another TRMM product 3B43. The 3B43 product combines the estimates generated by 3B42 and global gridded rain gauge data from the Climate Assessment and Monitoring System (CAMS), produced by NOAA's Climate Prediction Centre and/or global rain gauge product, produced by the Global Precipitation Climatology Centre (GPCC). The output is gridded rainfall with a spatial resolution of 0.25° for each month. The scaling of the 3-h product 3B42 to match the monthly rain gauge analyses product leads to a delay of at least one month until this product is available as data source for precipitation.

Station data are used as third meteorological data source. Especially in regions with weak infrastructure, where no automatic data recorders are used, the delay can increase up to one year or more until data are collected, digitized, and made available. The simulation period for this study is the year 2004. For 2004 station data from the Meteorological Services Department in Ghana and the GLOWA-Volta project are available at 20 locations in Ghana. In Burkina Faso observations of only two stations of the GLOWA-Volta project are available. Fig. 1 shows the location of the stations.

4.1. Comparison/validation of the different meteorological data sources

Fig. 2 shows the spatial distribution of the annual precipitation for 2004 resulting from the meteorological simulations for domain 2 (27×27 km^2) and domain 3 (9×9 km^2) and the TRMM product 3B42. The general spatial distribution of annual precipitation of the meteorological simulations with domain 2 and domain 3 are comparable and show a strong North–South gradient and an additional minimum along the shore South of Lake Volta. Compared to the results of domain 2, the patterns are refined in domain 3. The patterns are in good agreement with the mean annual rainfall (1951–1989) map from ORSTOM (1996). The spatial distribution of the TRMM product ($0.25° \times 0.25°$) is comparable with the results of domain 2, which is approximately on the same scale. But North of Lake Volta and in Burkina Faso the annual precipitation of the TRMM product is approximately 25% higher. For validation of the meteorological simulations scatter plots of the monthly precipitation amount for domain 2, domain 3 and the TRMM product 3B42 versus the observed monthly sums at 22 available stations are shown in Fig. 3. The 22 stations are subdivided into four regions: the coast (blue triangles), between latitude 7.5° and 8° (green stars), North of Lake Volta between latitude 8.5° and 9.5° (brown squares) and North Ghana and South Burkina Faso between latitude 10.0° and 11.5° (grey diamonds). For the calculation of the simulated precipitation at each station, the results of four neighboring grid points were interpolated using the inverse distance weighting method. The scatter plots of the MM5 simulations (Fig. 3a and Fig. 3b) show a fairly well agreement with partly under- and overestimations of the monthly precipitation sums. Compared to domain 2, domain 3 tends toward overestimating rain intensive months. However, in total domain 2 underestimates the monthly sums about 25% (regional range: −35% to −5%), and

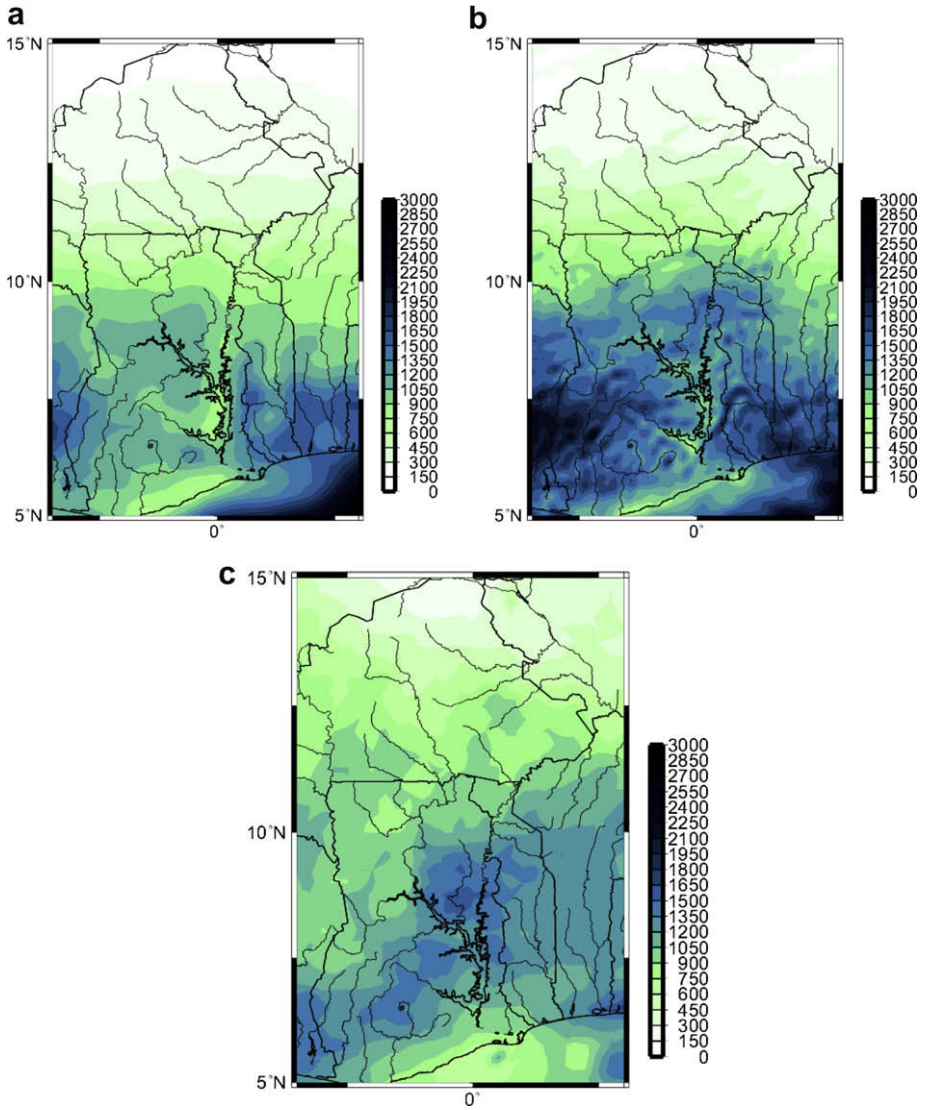

Fig. 2. Annual precipitation (mm) for 2004 using: (a) the meteorological model for domain 2 (27×27 km^2), (b) domain 3 (9×9 km^2) and (c) the TRMM product 3B42.

for domain 3 the regional differences between −15% and 20% compensate each other to an overestimation of 1%. The mean coefficients of determination R^2 (square of Pearson correlation coefficient) for all four regions, which are given in Table 1, indicate a better simulation result for domain 3 in the northernmost region, but for the remaining area domain 2 provides better performance. The scatter plot of the scaled TRMM product 3B42 shows a good performance with a total overestimation of 12% (regional range: −7% to 29%) compared to observations. Compared to the MM5 results, the coefficients of determination given in Table 1 are better. For the hydrological simulations in the White Volta catchment especially the results in Burkina Faso and northern Ghana are important. Comparing simulation results derived from meteorological models with point measurements (stations), it has to be considered that models are only able to simulate precipitation averages on a scale that is two to four times the model resolution (Pielke, 2002). This is particularly relevant for regions with a high spatial variability such as the White Volta catchment.

4.2. Hydrological simulations

The second step is the application of the above described different meteorological data sources in hydrological simulations on a daily time step. Results of the hydrological simulations for the three different meteorological input data sources are given in Figs. 4–6, which show the time series of precipitation (upper plot) and the time series of routed and measured discharge (lower plot) for the station Pwalugu in North Ghana for each meteorological data source. The discharge hydrographs available at near real time (Fig. 4) show comparable and satisfying results for both domains. Similar differences as in the precipitation time series of domain 2 and domain 3, can also be found in the discharge hydrographs. Compared to MM5 driven simulations, the simulation results of the TRMM product 3B42 (Fig. 5) show a different course of the precipitation time series, e.g. the precipitation maximum is in June, which hampers a correct simulation of the discharge hydrograph. The performance of the hydrological simulations driven by station data is satisfying and comparable to the results achieved with the meteorological model output. The main differences are the event in May which is less pronounced in the simulations driven by meteorological model output and the maximum peak end of August which is slightly overestimated respectively underestimated depending on the meteorological input data source. To compare the performance of the hydrological simulations of the applied meteorological input data sources, Nash–Sutcliffe model efficiencies are calculated

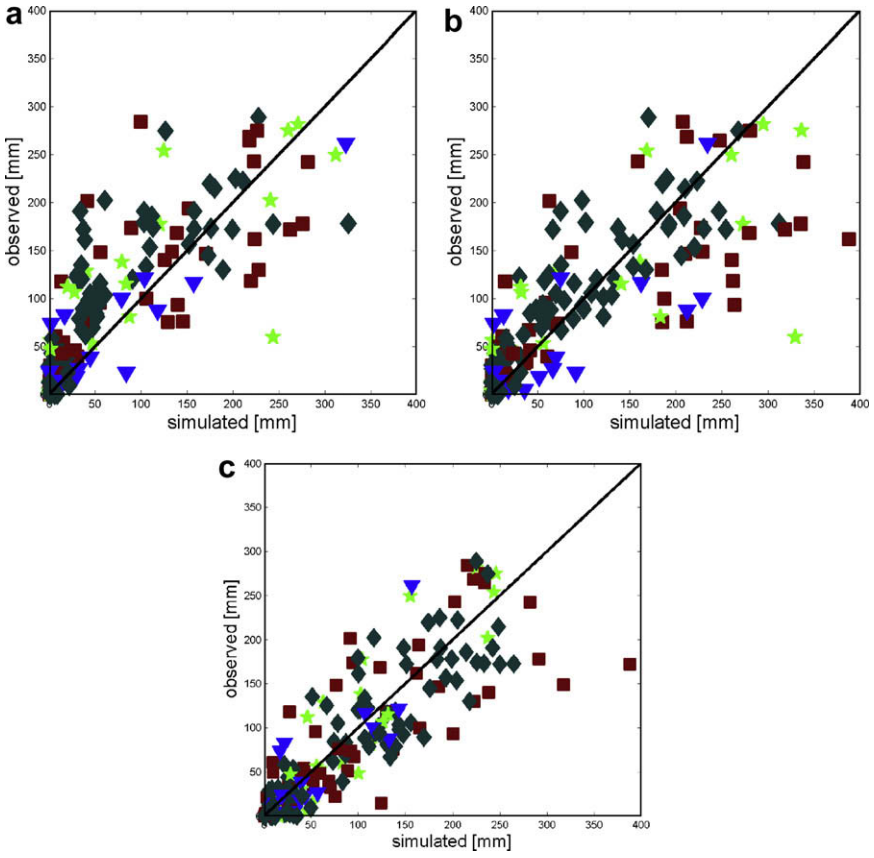

Fig. 3. Scatter plots of simulated vs. observed monthly precipitation for 2004. The 22 stations are subdivided into four regions: the coast (blue triangles), between latitude 7.5° and 8° (green stars), North of Lake Volta between latitude 8.5° and 9.5° (brown squares) and North Ghana and South Burkina Faso between latitude 10.0° and 11.5° (grey diamonds). The plot show the results of the meteorological model for domain 2 (a) and domain 3 (b), and the results of the TRMM product 3B42 (c).

Table 1
Mean coefficients of determination (R^2) of the investigated meteorological data sources: meteorological model output for domain 2 and domain 3 and the TRMM product 3B42 with respect to observations for 2004

Latitude (°)	Domain 2	Domain 3	TRMM 3B42
10.0–11.5	0.75	0.83	0.86
8.5–9.5	0.72	0.68	0.67
7.5–8.0	0.71	0.69	0.84
5.5–6.5	0.83	0.74	0.92

The stations are subdivided into four regions.

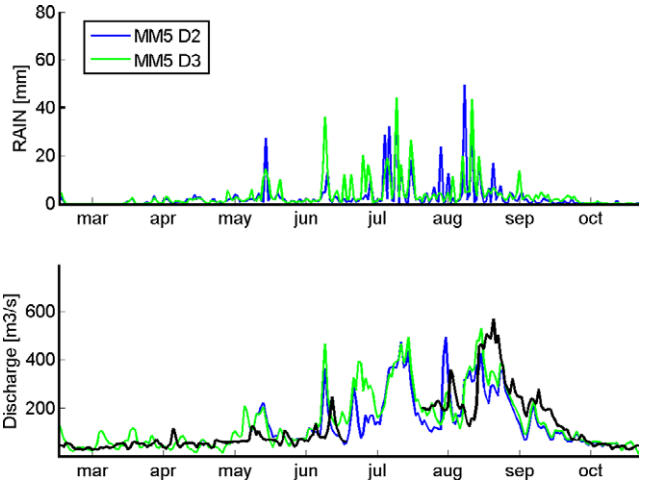

Fig. 4. Time series of precipitation and simulated vs. measured (black) discharge at Pwalugu for 2004 using the results of the meteorological model for domain 2 (blue) and domain 3 (green) as meteorological input data source which is available at near time.

with the logarithms of the runoff values, because the objective is to simulate the entire discharge hydrograph without special emphasis on peak flows. For Pwalugu the Nash–Sutcliffe coefficients for the simulations driven by the meteorological model output are similar: 0.67 for domain 2 and 0.69 for domain 3. The performance of the TRMM product as meteorological input data source is low (0.20). The Nash–Sutcliffe coefficient for the simulations driven by station data is 0.60, which is slightly less than the performance of the simulations with the meteorological model output, mainly due to the overestimation of the event in May. Additionally to Pwalugu only two further sub-catchments are available: the headbasin Nasia and the outlet of the complete catchment Nawuni. The Nash–Sutcliffe coefficients range for the simulations driven by (a) the meteorological model outputs between 0.31 and 0.72, by (b) the TRMM product 3B42 between 0.20 and 0.67, and by (c) station data between 0.60 and 0.88. In this study the TRMM product 3B42 does not improve the results of the hydrological simulations compared to the simulations driven by meteorological model outputs, although the coefficients of determination of the monthly precipitation are better. The main reason of the discharge overestimations is the higher precipitation amounts of the TRMM product 3B42 compared to the MM5 results in Burkina Faso. This overestimation is not considered in the coefficient of determination values due to missing observations.

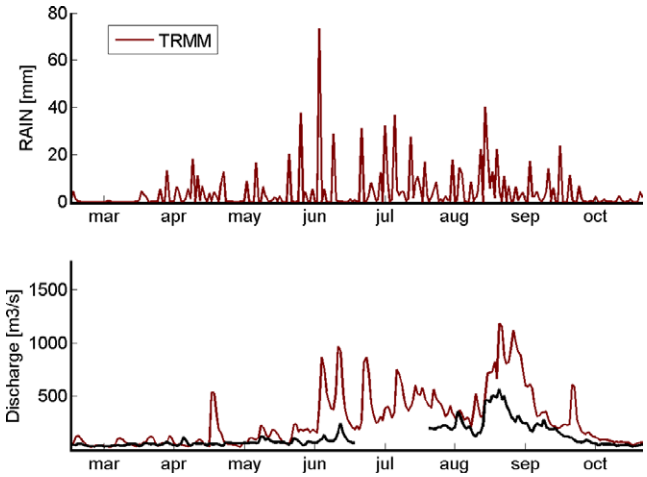

Fig. 5. Time series of precipitation and simulated vs. measured (black) discharge at Pwalugu for 2004 using the results of the TRMM product 3B42 as meteorological input data source which is available with approximately one month delay.

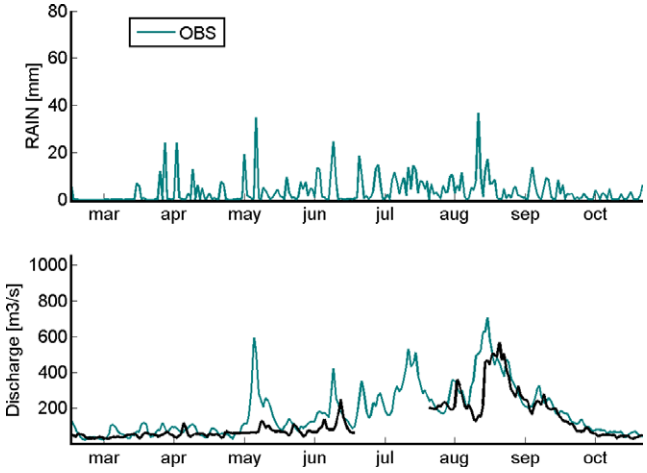

Fig. 6. Time series of precipitation and simulated vs. measured (black) discharge at Pwalugu for 2004 using station data as meteorological input data source which is available with approximately one year delay in this region.

5. Land surface data sources

In the second part, the influence of satellite-derived land surface data on hydrological simulations is investigated. Commonly tabulated standard literature data depending on land use classes are incorporated into the modeling process through the land use grid. In this study we substitute the static parameterization of the land surface parameters albedo and leaf area index (LAI) by dynamic estimates based on land surface products from the MODIS instrument. Station data are used as meteorological data source.

5.1. MODIS LAI and albedo products

The MODerate resolution Imaging Spectroradiometer (MODIS) instrument launched onboard Terra (EOS-AM1) and Aqua (EOS-PM1) in 2000 and 2002, respectively, is a part of NASA's Earth Observing Systems (EOS) (Justice et al., 2002). A near-polar sun synchronous orbit at 705 km and a swath of 2300 km allow global coverage within one to two days. Each instrument has 36 spectral bands ranging from the visible to the thermal infrared with near-nadir spatial resolutions of 250, 500, and 1000 m (Guenther et al., 2002; Wolfe et al., 2002). To investigate terrestrial ecological processes, the MODIS Land (MODLand) science team offers a wide range of value-added products based on MODIS calibrated radiances (Justice et al., 1998). This study employed 8-day products of the LAI (MOD15A2) and 16-day standardized albedo composites (MOD43B3) of MODIS collection 4.

The LAI is defined as total one-sided leaf area per unit ground surface (Privette et al., 2002). The standard procedure uses look-up-tables of simulated values generated by radiation transfer models (Knyazikhin et al., 1998). For collection 4, processing is separated in six biome-classes representing the most dominant vegetation types on a global scale because the retrieval of the LAI from spectral radiances strongly depends on leaf properties and vegetation structure (Myneni et al., 1997). Even though designed to include the first seven MODIS channels ranging from the visible blue to the short wave infrared (Knyazikhin et al., 1998), current collection 4 data only consider red and near infrared wavelengths due to several difficulties such as noise in the blue channel caused by atmospheric influences. If the standard routine fails because of insufficient cloud-free observations a back-up algorithm estimates LAI utilizing known empirical regressions between normalized difference vegetation index (NDVI) and LAI (Myneni et al., 2002).

The MOD43B3 product belongs to the group of bidirectional reflectance distribution function (BRDF)/albedo products and contains black-sky (directional hemispherical) and white-sky (bihemispherical) albedo for the first seven MODIS channels (Schaaf et al., 2002). A constant situation of the earth surface is assumed for the 16-day compositing period, and values are adjusted to local solar-noon angles. The so-called *RossThickLiSparse-Reciprocal* model, a linear kernel function, is used for the derivation of single band albedos (Lucht et al., 2000). In addition, a broadband albedo from 0.3 to 4.0 μm is computed by integrating narrow band albedos (Liang, 2000). This study employed broadband white-sky albedo composites.

MOD15A2 and MOD43B3 products are distributed as gridded 1 km spatial resolution datasets in the Sinusoidal projection and were reprojected to UTM zone 30N in this study. The unique concept of quality assurance and MODIS product validation (Roy et al., 2002) allowed the generation of science-quality time series.

5.2. MODIS time series generation

All MODIS products comprise additional so-called quality assurance science data sets (QA-SDS) for error estimation, atmospheric inferences, algorithms, or important surface characteristics (Roy et al., 2002). MODIS quality layers indicate crucial information such as cloud coverage, which is not reflected in the actual dataset (Colditz et al., 2006). Besides a so-called mandatory flag, a general quality indicator available for all products, additional product-specific quality assurance flags specify the usability of each dataset. The QA-SDS of the MOD15 product indicates potential cloud coverage, the algorithm used for LAI estimation, and possible detector failures. An additional QA-SDS provides important surface state information, which were generated by upstream data production (level 2 and 3) including a land/water mask, more specific cloud information including cloud shadow, and aerosol retrieval (Myneni et al., 2002). Similarly, detailed quality estimators are contained in the albedo product, in which the first part focuses on general issues such as mean solar angle, land/water, or snow, and the latter part on band-specific error estimates (Schaaf et al., 2002).

The time series generator (TiSeG, Colditz et al., in press) was used to analyze the QA-SDS of gridded MODIS products (Level 2G, 3, and 4). The interactive software computes and visualizes the data availability according to user-defined quality specifica-

tions. Two critical indices, the number of invalid pixels and the maximum gap length, are computed and displayed spatially and temporally. The number of invalid pixels is a general indication of data availability. The maximum gap length computes the longest period of invalid data. Next, pixels indicated as invalid data can be either masked or interpolated with spatial or temporal approaches. A thorough discussion of TiSeG, its functionalities, design, and performance is provided in Colditz et al. (in press).

As an example LAI time series processing is shown. The LAI time series generation with TiSeG involved a quality analysis followed by a linear temporal interpolation of all pixels which did not have good or acceptable quality. In total, the selected settings resulted in 70% pixels acceptable for interpolation. All pixels belonging to an internal mask of water, urban, and non-vegetated pixels are excluded from LAI processing. For a single pixel the respective time series contains between 0 and 25 invalid values (Fig. 7). Except for better conditions in the northernmost portion the spatial distribution of invalid pixels is nearly homogeneous throughout the White Volta catchment (Fig. 8a). The temporal analysis reveals that most invalid pixels occurred in the wet season between March and September (Fig. 9). The latter shows the seasonality with a long-lasting rainy period and substantial cloud coverage throughout the summer. The frequent drops in the

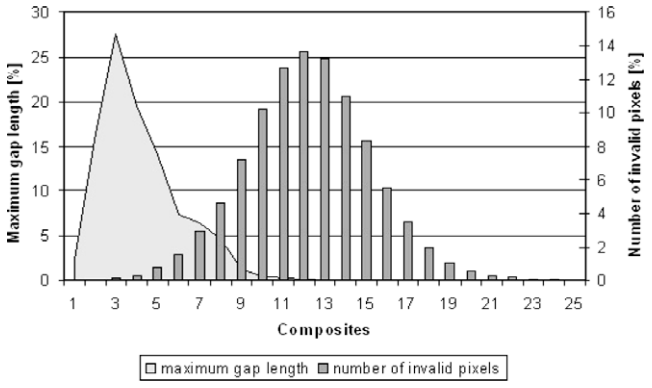

Fig. 7. Histogram of maximum gap length (bright filled area) and number of invalid pixels (dark columns) for LAI time series.

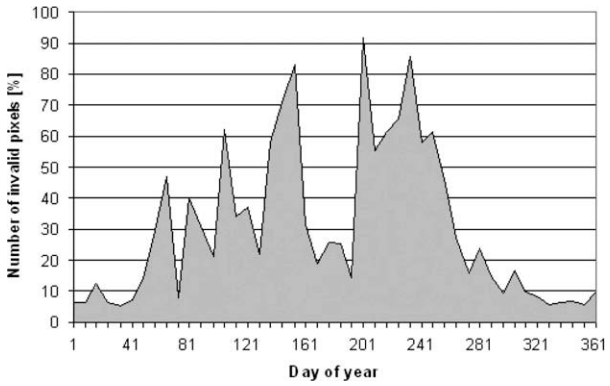

Fig. 9. Temporal plot of the number of invalid LAI pixels in percent.

graph, however, indicate that the resulting data gaps are comparatively short. The maximum gap to be interpolated is lower than eight composites for more than 85% of the entire catchment (Fig. 7) and the spatial view depicts a decreasing trend of the maximum gap towards less cloudy conditions in the northern area (Fig. 8b).

For the dominating biomes, savannas in the South as well as grassland/cereal crops and broadleaf crops in the northern part of the catchment (Fig. 10a), the average LAI time series are depicted in Fig. 10b. Changes resulting from temporal interpolation with respect to original data are highlighted. The dashed lines, representing the original data, clearly show inaccuracies which were excluded with the quality analysis using TiSeG (solid lines). Outliers in the late wet season are eliminated. The interpolated LAI profiles represent the expected phenological development starting to increase with the beginning of the wet season.

5.3. Results of water balance estimations using satellite-derived land surface data

The MODIS albedo and LAI time series are aggregated to monthly means for the hydrological simulations. Comparisons between standard literature tabulated- and MODIS values are shown for LAI in Fig. 11 and for albedo in Fig. 13, where monthly MODIS data are averaged to quarterly mean.

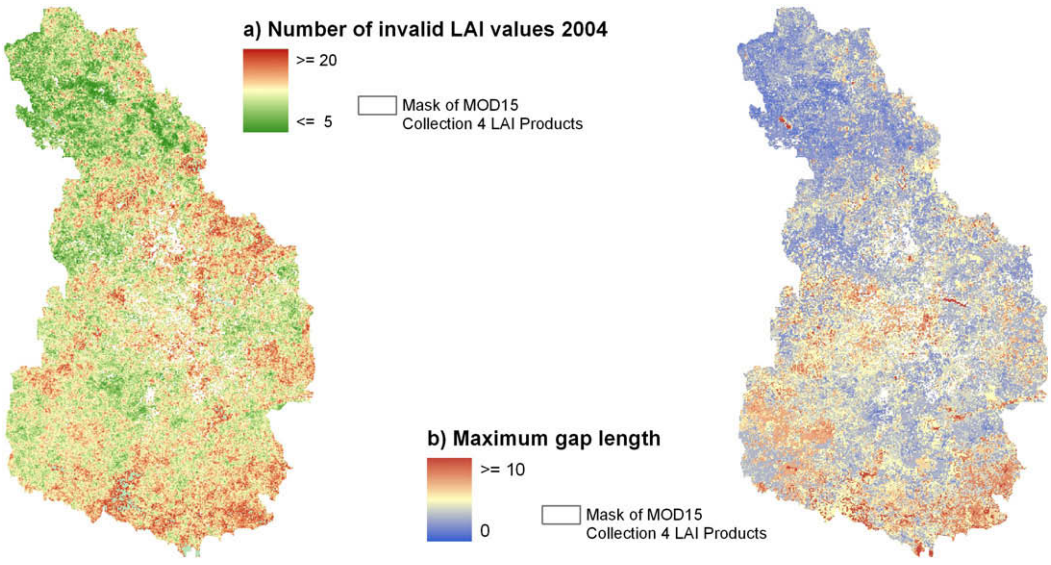

Fig. 8. Spatial quality analysis with TiSeG, (a) number of invalid LAI values, (b) maximum gap length.

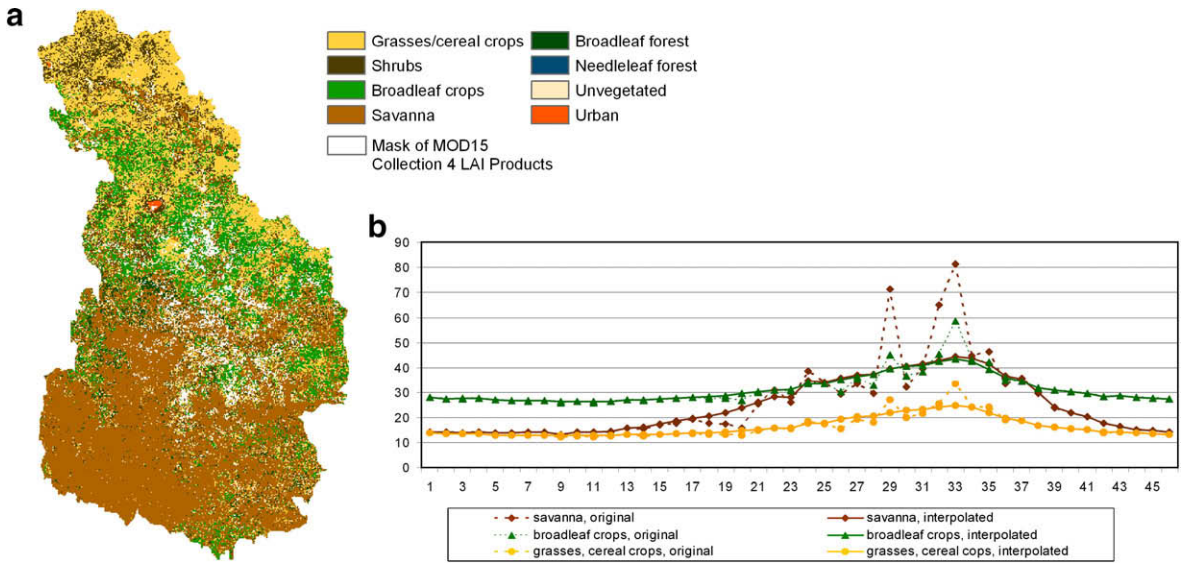

Fig. 10. (a) The biome map of the White Volta catchment and (b) original (dashed lines) and TiSeG-corrected (solid lines) average LAI (multiplied by factor 10) plots for dominating biomes savannah, broadleaf crops, and grassland/cereal crops.

5.4. LAI data comparison

For the LAI two seasons were defined for the hydrological simulations with tabulated land surface parameter values: a dry season between November and April with LAI values of mostly 0.5 in the northern and 1.5 in the southern part of the catchment and a rainy season between May and October with corresponding LAI values of 1.5 and 2.5 (see Fig. 11a) (Fensholt et al., 2004; Asner et al., 2003). The 3-month averaged LAI values of MODIS (Fig. 11b) are relatively constant around 0.5 between January and March within the entire basin. The LAI values start to increase according to expected phenological development beginning with the rainy season starting from the South (see also Fig. 10b). During the rainy season between July and September the LAI values reach their maxima. With the beginning of the dry season between October and December the LAI values decrease from the North. The temporal development of the LAI values is more distinctive in the southern and central part of the catchment. The comparison of Fig. 11a and b shows that the temporal development of the LAI is not sufficiently represented by two seasons with static values. In comparison to MODIS LAI, the tabulated values overestimate the LAI during the dry season basin-wide around 50% and underestimate it during the rainy season about 10% in the southern part of the basin.

5.5. Impact of MODIS LAI on water balance estimation

Results of the hydrological simulations using static and dynamic LAI data sources are shown as annual differences of actual evapotranspiration and total discharge in Fig. 12. The differences are defined as the results obtained by the hydrological simulations using tabulated values minus the results using MODIS values. The corresponding differences calculated as (a) relative root mean squared error (RMSE) and (b) relative annual differences are given for both variables in three different scales: total catchment-, sub-catchment- and local scale ($10 \times 10\,km^2$) in Table 2.

Fig. 12 shows that the differences of actual evapotranspiration are very heterogeneous in space with positive and negative differences in almost all sub-catchments. Because these differences compensate each other on catchment scale, the relative RMSE amounts to 5% for the total catchment. For the total discharge the spatial distribution of the differences is similar but opposite signs and larger magnitudes of relative differences on all three scales were calculated. The relative annual difference for the total catchment is +3%, but the relative RMSE amounts to 10%. In general, the hydrological simulations using MODIS LAI values result in higher annual evapotranspiration which finally leads to lower total discharge sums for 2004. Variations mainly occur in the South where literature values underestimate the vegetation cover and leaf area during the rainy season consequently resulting in lower evapotranspiration.

5.6. Albedo comparison

In WaSiM-ETH the albedo is time-invariant which results in one value per land use class (Grell et al., 1994). Fig. 13a and b shows a North–South gradient of the albedo values. For the MODIS albedo grid the gradient is larger and also more heterogeneous in the spatial dimension. During the rainy season (July–September) the MODIS albedo grid is more homogenous compared to the rest of the year. However, all seasonal aggregations depict similar spatial patterns of MODIS albedo which shows the stability of the parameter confirming the time-invariance of the albedo assumed in WaSiM-ETH. The spatially (White Volta basin) and temporally (year 2004) averaged MODIS albedo value is 0.19 compared to 0.23 using standard literature values. A further benefit of MODIS data is the increased level of detail in the spatial dimension.

5.7. Impact of MODIS albedo on water balance estimation

Results of the hydrological simulations using the two different albedo data sources are shown as annual differences of actual evapotranspiration and total discharge in Fig. 14. The corresponding RMSE and relative annual differences are given for both variables in the three different scales in Table 3.

Fig. 14 shows that the differences are again very heterogeneous in space. In almost all sub-catchments positive and negative differences occur which compensate each other to slightly negative values on sub- and catchment scale. The relative RMSE with 3% for the total catchment is also quite small. For the total

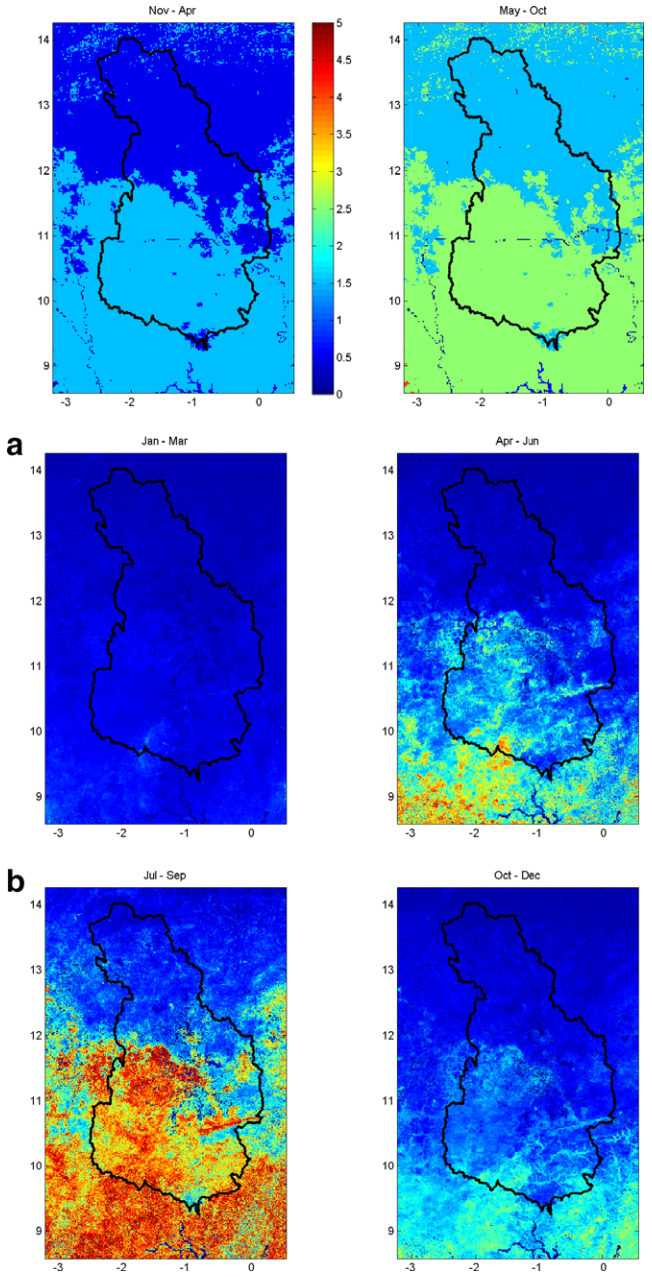

Fig. 11. LAI grid of the White Volta catchment using (a) static tabulated values and (b) dynamic MODIS estimates averaged to 3-month means.

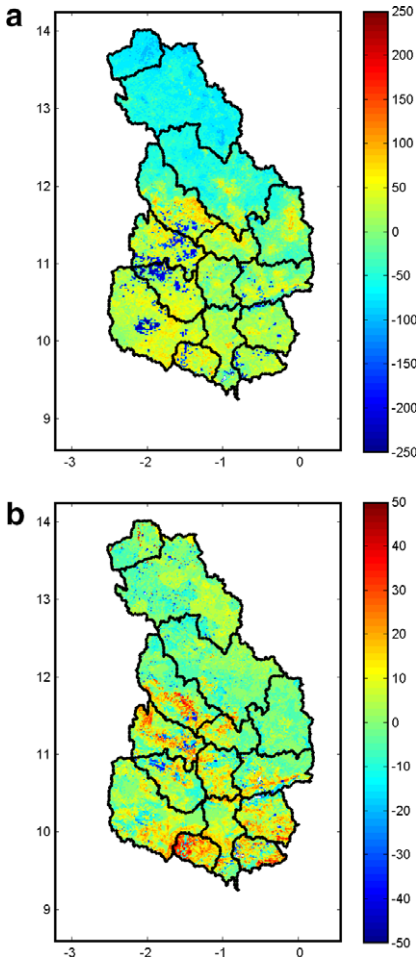

Fig. 12. Annual differences of (a) annual actual evapotranspiration (mm) and (b) total discharge (mm) for 2004 defined as results obtained by the hydrological simulations using tabulated values minus the results using MODIS LAI data.

Table 2
Percentage of relative RMSE (a) and relative annual differences (b)

	a ET (%)	Total Q (%)
(a)		
Total catchment	+5.0	+9.8
Sub-catchment	+3 to +8	+3 to +19
Local scale (10 × 10 km)	+1 to +13	+1 to +48
(b)		
Total catchment	−0.2	+3
Sub-catchment	−7 to +3	0 to +17
Local scale (10 × 10 km)	−11 to +7	−14 to +30

The results were obtained by hydrological simulations using tabulated LAI values minus the results using LAI of MODIS data for 2004.

discharge the spatial distribution is similar but opposite signs and larger magnitudes of the relative differences on all three scales were calculated. The relative annual difference for the total catchment is +6%, and the relative RMSE amounts to 11%. In general, the hydrological simulations using MODIS albedo values result in higher annual evapotranspiration and lower total discharge sums for 2004.

In summary, this study indicates that satellite-derived LAI and albedo impact the simulation results of water balance estimations. Furthermore, results of this study suggest that satellite-derived land surface information is of particular importance if local scale water budgets are required for decision making. However, if catchment or sub-catchment aggregated water balance estimates are sufficient, the impact is of minor importance.

6. Conclusions

Water balance estimations were performed for the White Volta catchment applying three different meteorological input data sources: (a) the results of a mesoscale meteorological model which are available near real time, (b) the TRMM product 3B42 with approximately one month delay and (c) station data with a delay of one year or more in this region. For the validation of meteorological model output and the TRMM product, monthly scatter plots and coefficients of variation were analysed. In this study the TRMM

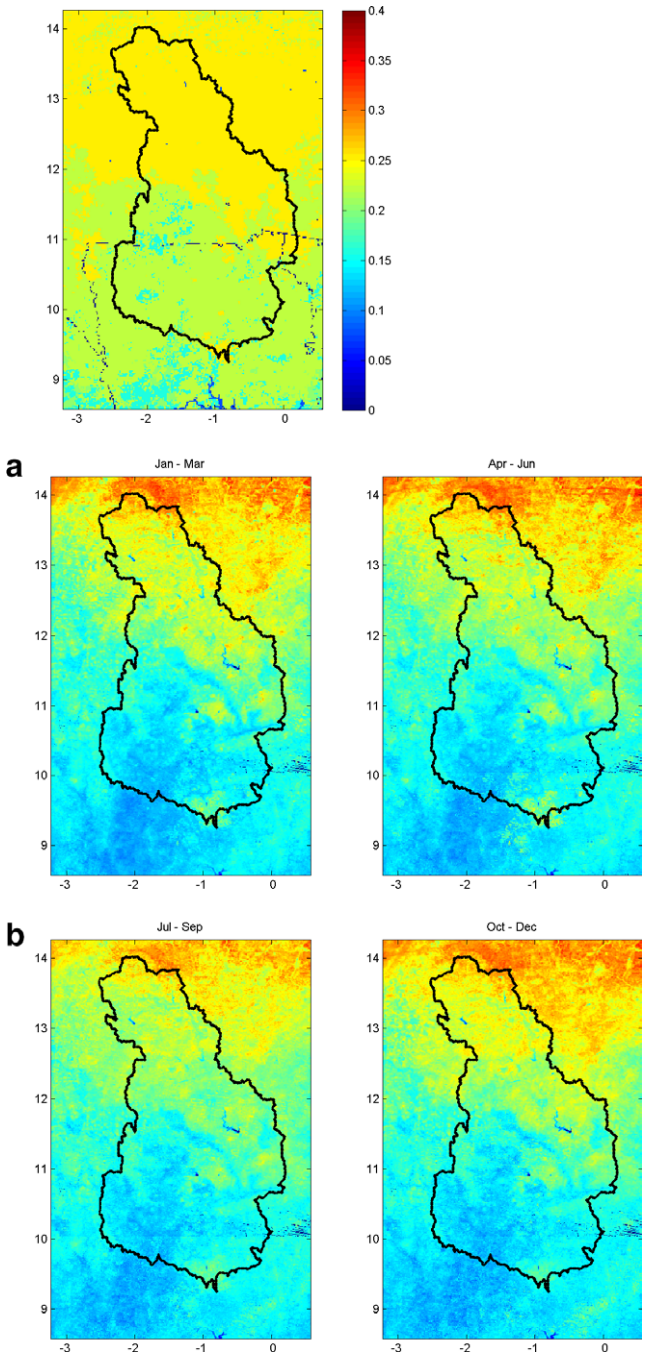

Fig. 13. Albedo grid of the White Volta catchment using (a) static tabulated values and (b) dynamic MODIS estimates averaged to 3-month means.

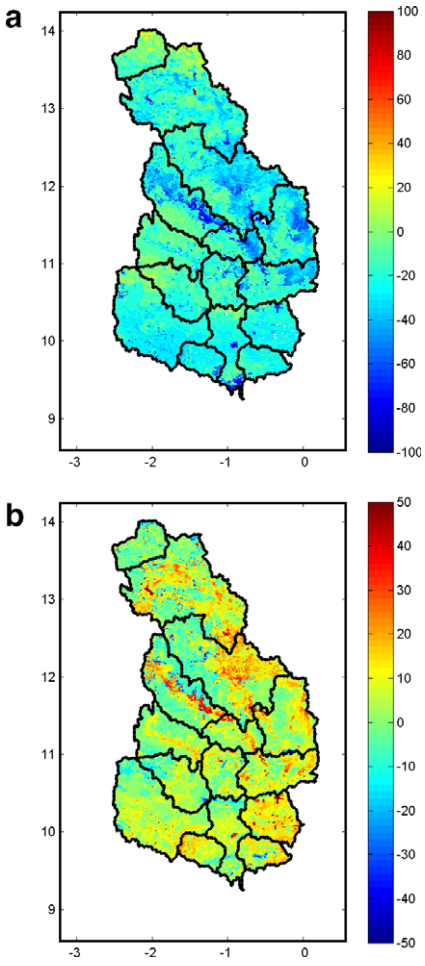

Fig. 14. Annual differences of (a) annual actual evapotranspiration (mm) and (b) total discharge (mm) for 2004 defined as results obtained by the hydrological simulations using tabulated values minus the results using MODIS albedo data.

Table 3
Percentage of relative RMSE (a) and relative annual differences (b)

	a ET (%)	Total Q (%)
(a)		
Total catchment	+2.6	+11
Sub-catchment	+1 to +4	+4 to +15
Local scale (10 × 10 km)	0 to +8	+2 to +42
(b)		
Total catchment	−2	+6
Sub-catchment	−2 to 0	0 to +14
Local scale (10 × 10 km)	−7 to +2	−10 to +30

The results were obtained by hydrological simulations using tabulated albedo values minus the results using albedo of MODIS data for 2004.

product 3B42 does not improve the results of the hydrological simulations compared to the simulations of meteorological models. This issue will be analysed further for the coming years. It is concluded that the meteorological model is able to provide the required meteorological input data for near real time hydrological simulations in reasonable quality. These simulations, however, require substantial CPU and storage capacities. This is not the case for the TRMM products, which, however, only provide precipitation data for the hydrological simulations, and no additionally required meteorological fields.

In the second part of the study, water balance estimations were performed using two different land surface data sources for albedo and LAI: (a) tabulated, standard literature values and (b) MODIS products. The MODIS products for LAI (MOD15A2) and albedo (MOD43B3) were processed to annual time series. Low quality observations were identified using the accompanying pixel-level quality assurance dataset and interpolated with linear temporal interpolation. The results of the hydrological simulation show that differences in the spatial distribution of water balance variables occur on local scale, but they decrease on sub-catchment and catchment scale. Furthermore, remote sensing products incorporate land surface processes, in particular vegetation dynamics, into hydrological simulation.

This study showed that the integration of atmospheric modeling and satellite-derived land surface data can significantly en-

hance the quality of water balance estimations in the West African White Volta Basin. The suggested approach can be generally concluded as valuable input for hydrological decision making in regions with few meteorological field measurements and sparse information on vegetation- and soil-dependent properties.

Acknowledgements

This work was funded by the BMBF (German Ministry of Education and Research) through the project GLOWA-Volta (http://www.glowa-volta.de). The collaboration with the Hydrological- and Meteorological Services Department in Ghana is gratefully acknowledged. The TRMM data used in this study were acquired as part of the Tropical Rainfall Measuring Mission (TRMM).

The MODIS data used in this study were acquired as part of the NASA's Earth Science Enterprise. The algorithms were developed by the MODIS Science Teams. The data were processed by the MODIS Adaptive Processing System (MODAPS) and Goddard Distributed Active Archive Center (DAAC), and are archived and distributed by the Goddard DAAC.

References

Asner, G., Scurlock, J., Hicke, J., 2003. Global synthesis of leaf area index observations: implications for ecological and remote sensing studies. Global Ecology and Biogeography 12, 191–205.

Chen, F., Dudhia, J., 2001. Coupling an advanced land-surface/hydrology model with the Penn State/NCAR MM5 modeling system. Part I: model implementation and sensitivity. Monthly Weather Review 129, 569–585.

Chen, J.M., Chen, X., Ju, W., Geng, X., 2005. Distributed hydrological model for mapping evapotranspiration using remote sensing inputs. Journal of Hydrology 305, 15–39.

Colditz, R.R., Conrad, C., Wehrmann, T., Schmidt, M., Dech, S.W., 2006. Generation and assessment of MODIS time series using quality information. In: IEEE International Conference on Geoscience and Remote Sensing, 2006. IGARSS 2006, Denver, CO, pp. 779–782.

Colditz, R.R., Conrad, C., Wehrmann, T., Schmidt, M., Dech, S.W., in press. TiSeG – a flexible software tool for time series generation of MODIS data utilizing the quality assessment science data set. IEEE Transactions on Geoscience and Remote Sensing.

Fensholt, R., Sandholt, I., Schultz Rasmussen, M., 2004. Evaluation of MODIS LAI, fAPAR and the relation between fAPAR and NDVI in a semi-arid environment using in situ measurements. Remote Sensing of Environment 91, 490–507.

Friesen, J., 2003. Spatio-temporal patterns of rainfall in Northern Ghana. Diploma Thesis, University of Bonn, Center for Development Research (ZEF), Bonn.

Grell, G., Dudhia, J., Stauffer, D., 1994. A description of the fifth-generation Penn State/NCAR mesoscale model (MM5). NCAR Technical Note, NCAR/TN-398+STR, Boulder/USA.

Guenther, B., Xiong, X., Salomonson, V.V., Barnes, W.L., Young, J., 2002. On-orbit performance of the Earth Observing System Moderate Resolution Imaging Spectroradiometer; first year of data. Remote Sensing of Environment 83 (1–2), 16–30.

Hayward, D., Oguntoyinbo, J., 1987. Climatology of West Africa. Hutchindson.

Hong, S., Pan, H., 1996. Nonlocal boundary layer vertical diffusion in a medium-range forecast model. Monthly Weather Review 124, 2322–2339.

Huffman, G.J., Adler, R.F., Rudolph, B., Schneider, U., Keehn, P., 1995. Global precipitation estimates based on a technique for combining satellite-based estimates, rain gauge analysis, and NWP model precipitation information. J. Clim. 8, 1284–1295.

Jung, G., 2006. Regional climate change and the impact on hydrology in the Volta Basin of West Africa. Ph.D. Thesis, Forschungszentrum Karlsruhe and University of Augsburg, Garmisch-Partenkirchen, 159 p.

Jung, G., Kunstmann, H., 2007. High resolution regional climate modelling for the Volta Basin of West Africa. Journal of Geophysical Research, doi:10.1029/2006JD007951.

Justice, C.O., Vermote, E.F., Townshend, J.R.G., DeFries, R.S., Roy, D.P., Hall, D.K., Salomonson, V.V., Privette, J.L., Riggs, G., Strahler, A.H., Lucht, W., Myneni, R.B., Knyazikhin, Y., Running, S.W., Nemani, R.R., Wan, Z., Huete, A.R., van Leeuwen, W.J.D., Wolfe, R.E., Giglio, L., Muller, J.-P., Lewis, P., Barnsley, M.J., 1998. The Moderate Resolution Imaging Spectroradiometer (MODIS): land remote sensing for global change research. IEEE Transactions on Geoscience and Remote Sensing 36 (4), 1228–1249.

Justice, C.O., Townshend, J.R.G., Vermote, E.F., Masuoka, E., Wolfe, R.E., el Saleous, N.Z., Roy, D.P., Morisette, J.T., 2002. An overview of MODIS land data processing and product status. Remote Sensing of Environment 83 (1–2), 3–15.

Kleinn, J., 2002. Climate change and runoff statistics in the Rhine Basin: a process study with a coupled climate-runoff model. Ph.D. Thesis, ETH Zuerich.

Knyazikhin, Y., Martonchik, J.V., Diner, D.J., Myneni, R.B., Verstraete, M.M., Pinty, B., Gobron, N., 1998. Estimation of vegetation canopy leaf area index and fraction of absorbed photosynthetically active radiation from atmosphere-corrected MISR data. Journal of Geophysical Research 103 (D24), 32239–32256.

Kunstmann, H., Jung, G., Wagner, S., Clottey, H., 2007. Integration of atmospheric sciences and hydrology for the development of decision support systems in sustainable water management. Journal of Physics and Chemistry of the Earth. doi:10.1016/j.pce.2007.04.01.

Liang, S., 2000. Narrowband to broadband conversions of land surface albedo: I Algorithms. Remote Sensing of Environment 76 (2), 213–238.

Lucht, W., Schaaf, C.B., Strahler, A.H., 2000. An algorithm for the retrieval of albedo from space using semiempirical BRDF models. IEEE Transactions on Geoscience and Remote Sensing 38 (2), 977–998.

Martin, N., van de Giesen, N., 2005. Spatial distribution of groundwater production and development potential in the Volta river basin of Ghana and Burkina Faso. Water International 30, 239–249.

Marx, A., 2007. Einsatz gekoppelter Modelle und Wetterradar zur Abschätzung von Niederschlagsintensitäten und zur Abflussvorhersage. Institut für Wasserbau, Universität Stuttgart, Mitteilungen. p. 160.

Monteith, J.L., 1975. Vegetation and the Atmosphere. Principles, vol. 1. Academic Press, London.

Myneni, R.B., Nemani, R.R., Running, S.W., 1997. Estimation of global leaf area index and absorbed PAR using radiative transfer models. IEEE Transactions on Geoscience and Remote Sensing 35 (6), 1380–1393.

Myneni, R.B., Hoffman, S., Knyazikhin, Y., Privette, J.L., Glassy, J., Tian, Y., Wang, Y., Song, X., Zhang, Y., Smith, G.R., Lotsch, A., Friedl, M.A., Morisette, J.T., Votava, P., Nemani, R.R., Running, S.W., 2002. Global products of vegetation leaf area and fraction absorbed PAR from year one of MODIS data. Remote Sensing of Environment 83 (1–2), 214–231.

Oguntunde, P., 2004. Evapotranspiration and complimentary relations in the water balance of the Volta basin: field measurements and GIS-based regional estimates. Ph.D. Thesis, Cuviliier Verlag Göttingen, pp. 15–16.

ORSTOM, 1996. Afrique de'l Ouest et Centrale Précipitations Moyennes Annuelles (Période 1951–1989). Laboratoire d'Hydrologie, B.P. 5045, 34032 Montepellier, Cedex, France.

Pielke, R., 2002. Mesoscale Meteorological Modeling. Academic Press.

Privette, J.L., Myneni, R.B., Knyazikhin, Y., Mukelabai, M., Roberts, G., Tian, Y., Wang, Y., Leblanc, S.G., 2002. Early spatial and temporal validation of MODIS LAI product in the Southern Africa Kalahari. Remote Sensing of Environment 83 (1–2), 232–243.

Reisner, J., Rasmussen, R., Bruintjes, R., 1998. Explicit forecasting of supercooled liquid water in winter storms using the MM5 mesoscale model. Quarterly Journal of the Royal Meteorological Society, 124B.

Richards, L., 1931. Capillary conduction of liquids through porous medium. Physics 1, 318–333.

Roy, D.P., Borak, J.S., Devadiga, S., Wolfe, R.E., Zheng, M., Descloitres, J., 2002. The MODIS Land product quality assessment approach. Remote Sensing of Environment 83 (1–2), 62–76.

Sandholt, I., Andersen, J., Dybkjaer, G., Nyborg, L., Lô, M., Rasmussen, K., Refsgaard, J.-C., Jensen, K.H., Touré, A., 2003. Integration of earth observation data in distributed hydrological models: the Senegal River basin. The Canadian Journal of Remote Sensing 29 (6), 701–710.

Schaaf, C.B., Gao, F., Strahler, A.H., Lucht, W., Li, X., Tsang, T., Strugnell, N.C., Zhang, X., Jin, Y., Muller, J.-P., Lewis, P., Barnsley, M.J., Hobson, P.D., Disney, M., Roberts, G., Dunderdale, M., Doll, C., d'Entremont, R.P., Hug, B., Liang, S., Privette, J.L., Roy, D.P., 2002. First operational BRDF, albedo nadir reflectance products from MODIS. Remote Sensing of Environment 83 (1–2), 135–148.

Schulla, J., Jasper K., 2000. Model Description WaSiM-ETH. ETH Zürich, Zurich, 166 p.

VBRP, 2002. Volta Basin Research Project Water Resources Management GIS Maps on the Volta Basin. Accra, Ghana.

Wagner, S., Kunstmann, H., Bárdossy, A., 2006. Model based distributed water balance monitoring of the White Volta catchment in West Africa through coupled meteorological–hydrological simulations. Advances of Geosciences 9, 39–44.

Wolfe, R.E., Nishihama, M., Fleig, A.J., Kuyper, J.A., Roy, D.P., Storey, J.C., Patt, F.S., 2002. Achieving sub-pixel geolocation accuracy in support of MODIS land science. Remote Sensing of Environment 83 (1–2), 31–49.